FULL-SCALE EXPERIMENTAL RESULTS ON THE MEAN AND TURBULENT BEHAVIOR OF ROOM VENTILATION FLOWS

J.S. Zhang, Ph.D.
Associate Member ASHRAE

G.J. Wu, Ph.D., P.E.
Member ASHRAE

L.L. Christianson, Ph.D., P.E.
Member ASHRAE

ABSTRACT

Experiments were conducted in a full-scale test room (18 by 24 by 8 ft [5.5 by 7.3 by 2.4 m]) for both isothermal and nonisothermal conditions. Based on the experimental data, this paper discusses (1) the statistical features of air velocity fluctuations including probability density functions and energy spectra; (2) the observed airflow patterns; and (3) the spatial distributions of mean velocity, turbulence intensity, kinetic energy of turbulence, and mean temperature. Special attention is paid to the effects of the diffuser air velocities and internal heat loads on the flow characteristics and to the differences between the diffuser jet region and the occupied region. The detailed experimental data are also useful for evaluating and improving numerical simulation models of room air motion.

INTRODUCTION

Understanding room air distribution is essential to the design of ventilation systems and control of room thermal and air quality conditions. Air velocities in occupied zones of a room directly affect the thermal comfort of occupants. The movement of air within a room also affects the release rate of heat and contaminants from sources and determines how the heat and contaminants distribute, thus affecting the air quality available to the occupants. In addition, proper air distribution can reduce the ventilation rate necessary for removing air contaminants and moisture, thus reducing building energy consumption. Study of room air distribution is important to many applications, including commercial and residential rooms, clean room manufacturing, electronic and computer rooms, biomedical research, hospital disease control, and greenhouse and animal agriculture (Christianson 1989).

Room air distribution is a complicated process. Researchers have developed a limited understanding through experimental measurements and numerical modeling. Research efforts have concentrated on high ventilation rate conditions (fully turbulent flow), isothermal conditions (no internal heat loads), limited, if any, internal obstructions (no furniture and equipment), and simple room geometries to simplify the problem. Realistic room ventilation flow usually has multiflow features, including high and low turbulence, which increase the complexity of both physical and mathematical modeling. Physical modeling is also complicated by the difficulty of air velocity measurements since low air velocities (< 50 fpm [0.25 m/s]) are involved.

Methods commonly used for investigating room air distribution are full-scale measurements, similitude model study, and numerical simulations. Measurements in full-scale rooms are essential to the understanding of room flow behavior, and the evaluations of indirect techniques such as similitude studies and numerical models, and are currently the only assured method of evaluating room airflow. However, it is generally expensive and inconvenient to conduct full-scale experiments, and the results can only be applied to rooms that are identical (at least very similar) to the prototype studied.

Similitude study involves experiments in a reduced-scale-model room and extrapolations of the results from this model room to its prototype. More important, similitude makes it possible to extrapolate experimental findings to a variety of rooms with similar geometry without the need for physical modeling of every prototype. The application of similitude to room airflow is limited by our knowledge of proper scaling methods for extrapolating the data. Knowledge of the regional characteristics of the room airflow, including its turbulent behavior, is necessary to the development of the scaling theory.

Numerical simulation involves mathematically modeling the room airflow and numerically solving the model. While complicated, it is in principle the most generalized method and thus is most convenient for predicting room airflows. However, advances in numerical modeling are limited by the lack of compatible, adequately detailed experimental data for model evaluation and by the lack of knowledge of room airflow characteristics, especially the turbulent flow features.

The objectives of this research were to improve the understanding of the mean and turbulent behavior of realistic room ventilation flows and provide experimental data for evaluating and improving numerical simulation models of room air motion.

Jianshun Zhang, Ph.D., is a research associate at the Institute for Research in Construction, National Research Council of Canada, Ottawa, Ontario. **G. Jeff Wu**, Ph.D., P.E., is an assistant professor at the University of Wisconsin, Madison. **Leslie L. Christianson**, Ph.D., P.E., is a professor and director of the Bioenvironmental Engineering Research Laboratory, University of Illinois, Urbana.

LITERATURE REVIEW

The following review is not meant to be exhaustive but to give a clear picture of the current status of full-scale studies of room ventilation flows.

Studies Conducted in the U.S.

Straub and Chen (1957) conducted more than 300 heating and cooling tests with a number of different diffusers, diffuser locations, airflow rates, return locations, and room heat loads. These data are valuable and have resulted in empirical equations for predicting the trajectory and centerline velocities of diffuser air jets that are still widely used (ASHRAE 1989).

Nevins and Miller (1972) studied room air movement extensively. They defined the air diffusion performance index (ADPI) to relate room air distribution to human comfort. They showed that ADPI could be related to room air diffuser characteristics, room size, and cooling load.

Hart and Int-Hout (1980) tested a perimeter linear air diffuser in a full-scale model office building and concluded that linear air diffusers can satisfy office building comfort needs without the need for a heat source on exterior window walls to prevent downward drafts from moving from the window to the occupied zone.

Fitzner (1981) conducted full-scale model experiments for an air-conditioned room. Fitzner showed that the airflow inside the room was mainly influenced by the form and location of the air diffuser, the air exchange rate, the cooling rate (which affects the thermal buoyancy effect), and the direction of introduced airflow with respect to gravity. The influence of air returns usually could be neglected. He also compared three types of diffusers in terms of gas concentration versus height and distance from a gas source.

Timmons (1984) used smoke to observe the flow pattern in a prototype building with cross-sectional dimensions of 25.3 by 6.7 ft (7.72 by 2.05 m). The fluid motion near the room exhaust approximated potential flow, while most of the room airflow was highly turbulent when the diffuser Reynolds number ($U_d w_d/\nu$) was smaller than 18,000. Airflow near the diffuser was not characterized in detail.

Zhang et al. (1992) conducted full-scale measurements for evaluating numerical models of room air motion. Measurements included detailed spatial distributions of air velocity, turbulent kinetic energy, turbulence intensity, and temperature. Profiles of mean velocity and turbulent kinetic energy were also measured at the diffuser; these are useful for specifying boundary conditions in compatible numerical simulations.

Studies Conducted Outside the U.S.

Researchers in other parts of the world have also measured airflow patterns in full-scale rooms. Baturin (1972) summarized information gained mainly by Russian researchers, which focused on industrial ventilation.

More recently, Melikov et al. (1988) and Sandberg (1989) measured air velocities and turbulence characteristics in full-scale rooms. These data, which focused on the occupied regions, are valuable for understanding room flow behaviors, especially its turbulence feature.

To evaluate several numerical simulation codes, researchers in Annex 20[1] of the International Energy Agency have measured velocities, temperatures, and turbulence velocity scales[2] in full-scale rooms. Measurements were conducted in several different laboratories for the same pre-specified room dimensions and configurations, heat load, and diffuser type. Measurements from different laboratories generally agree with each other, but some varied by ±40% and ±65% for average velocity and turbulence velocity scale, respectively, in the occupied zone (Whittle and Clancy 1991). The variations were attributed to the difficulties in achieving identical test conditions (e.g., thermal symmetry, supply air temperature, steady flow, and diffuser velocity profiles).

British agricultural engineers conducted a series of full-scale studies (Carpenter et al. 1972; Randall 1975; Randall and Battams 1979; Boon 1978). A corrected Archimedes number, which included the effect of diffuser and room dimensions and the discharge coefficient, was defined to characterize the jet trajectory and room airflow patterns. Critical values of the corrected Archimedes number were established to help the design of room air distribution.

Canadian researchers (Barber et al. 1982) proposed a jet momentum number to measure the energy contained in the diffuser jet relative to the room air volume. It was concluded that the jet momentum number should be higher than a minimum value to ensure sufficient mixing of the incoming air with the room air before the incoming air reaches the occupied zone. It was also found that there was a high correlation ($R > 0.85$) between the floor velocity and the jet momentum number (Ogilvie and Barber 1988).

These British and Canadian studies suggest that air velocity at a certain level or in a certain region of a room may be predicted based on one or two diffuser airflow indices such as the corrected Archimedes number or the jet momentum number.

EXPERIMENTAL FACILITY AND PROCEDURE

To investigate the various aspects of room air distribution, a room ventilation simulator was developed with several unique features—an outer room with an HVAC (heating, ventilating, and air-conditioning) system to

[1]Annex 20 is an international cooperative research group including room air motion and building environment studies experts from 12 European and North American countries.

[2]The turbulence velocity scale was defined as the standard deviation of velocity fluctuations by the Annex 20 researchers.

simulate different weather conditions by controlling the ambient air environment around the test room, an inner test room of modular design to facilitate changing room dimensions and configurations, an independent HVAC system for the inner test room to study different air supplies, an air delivery system capable of providing an airflow rate of 2 to 52 air changes per hour (ach); a uniform floor heating system of 48 controllable panels to simulate internal heat loads; a computer-controlled data acquisition and probe-positioning system to allow automatic measurements at precisely positioned locations; and a flow visualization system to record room airflow patterns. Additionally, computer software was developed for data analyses. Details can be found in Wu et al. (1990) and Zhang (1991).

Results presented in this paper are from a full-scale experimental setup shown in Figure 1. The test room has a continuous slot diffuser and a continuous slot exhaust. Measurements indicated that the flow inside the room was practically two-dimensional except very close to the two end walls (Zhang 1991). The internal heat load was simulated with the heating panels uniformly distributed on the floor surface.

Velocities and temperatures were measured at 205 locations (Figure 2) at the central section of the room with a hot-wire anemometer and a thermocouple, respectively. Additionally, smoke generated by titanium tetrachloride was used to visualize the room airflow patterns. Test conditions are listed in Table 1.

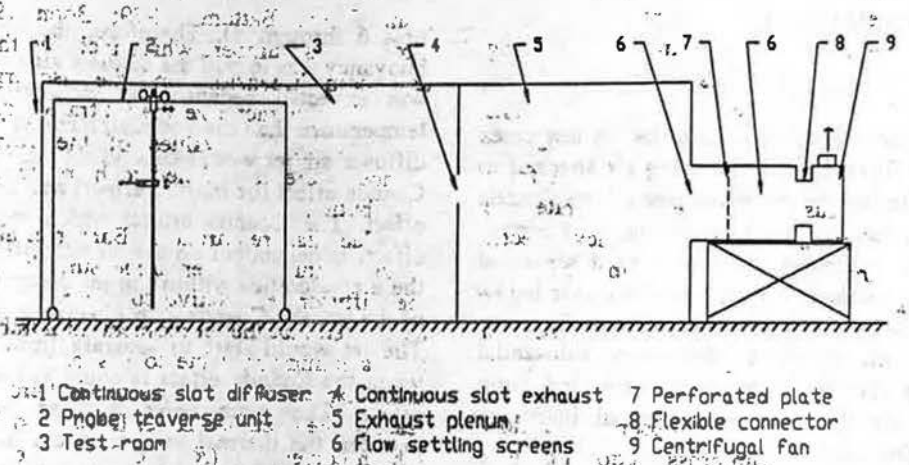

Figure 1 Experimental setup for the full-scale room (z direction is into the page).

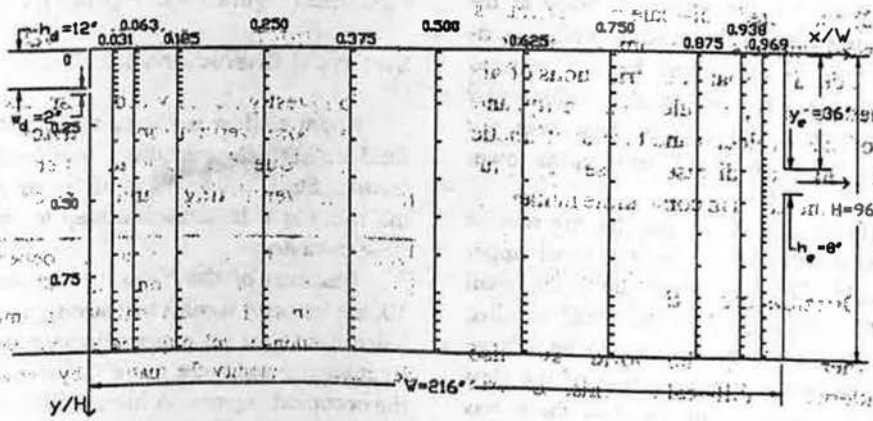

Figure 2 Probe locations for velocity and temperature measurements (z direction is into the page).

TABLE 1
Test Conditions

Test	U_d (fpm)	T_d (°F)	T_e (°F)	T_f (°F)	ΔT_{fd} (°F)	Re_d	Ar_{fd}	Q (ach)
P1	500	75	75	75	0	8193	0	27.9
P2	350	75	75	75	0	5735	0	19.5
P3	150	75	75	75	0	2458	0	8.6
P4	350	75.4	90.3	142.7	67.3	5735	0.0186	19.5
P5	350	73.9	83.8	121.8	47.9	5735	0.0135	19.5
P6	350	73.6	80.0	103.5	29.6	5735	0.0085	19.5

*w_d = 2 inches for all the tests.

RESULTS AND DISCUSSION

Flow Patterns

The common flow behavior among the six test cases (Figures 3 through 8) is that the incoming air attached to the ceiling after entering the room because of the Coanda effect. The air then traveled along the ceiling for a certain distance (called the attachment length) until it separated from the ceiling or reached the opposite wall. Air below the jet was entrained by the jet so that a reverse flow was formed below the jet. However, there were substantial differences among the six tests, which resulted from different diffuser air velocities and thermal buoyancy effects caused by the internal heat loads.

Effect of Diffuser Air Velocity At the highest diffuser air velocity (Figure 3), there was a strong primary recirculation eddy in the upper right corner and a secondary recirculation eddy in the lower left corner.

The flow pattern in the medium diffuser air velocity test (Figure 4) was very similar to that from the highest diffuser air velocity case, but the secondary eddy at the lower left corner was not clearly observed in the medium-velocity case. This may be explained by the reduced inertial effect due to the decrease in the diffuser air velocity. The momentum in the reverse flow was not enough to generate the strong secondary eddy in the lower left corner.

At the lowest diffuser velocity (Figure 5), the reverse flow below the diffuser jet occupied only a small upper portion of the flow field. This was again due to the small amount of momentum in the diffuser air jet, which resulted in much less entrained air. There appeared to be a large weak recirculation flow in the lower portion of the flow field due to molecular viscosity, but the flow there was essentially stagnant.

Effect of Thermal Buoyancy For a lower internal heat load, the diffuser air jet attached to the ceiling for a longer distance before it separated from the ceiling (Figures 6 through 8). Therefore, the effect of the thermal buoyancy was to pull the diffuser air toward the floor. This was expected because the incoming air had a lower temperature than the room air. The separation point of the diffuser air jet would depend on the balance between the Coanda effect (or inertial effect) and the thermal buoyancy effect. The Coanda effect, which represents the inertial effect, is dependent on the air velocities within the jet. As the air velocities within the jet decay along the trajectory of the jet, the Coanda effect becomes smaller and smaller. The jet would start to separate from the ceiling surface when the Coanda effect is equal to the thermal buoyancy effect. The Archimedes number represents the ratio between the thermal buoyancy and inertial effects and is therefore naturally used to characterize the room airflow patterns.

It was also observed that flow in the nonisothermal cases had stronger random behavior than in the isothermal cases. For the nonisothermal cases, flow observed at the same location but at different times had more directional variations (Figure 7 vs. Figure 4).

Statistical Characteristics

Room airflow involves turbulence. The movement of fluid el... turbulent flow field has a strong random feature. Statistical an... is of the air velocity signals within the room is a fundamental step toward understanding the flow behavior.

Features of the Velocity As shown in Figures 9 and 10, the velocity signals had strong random features. The air velocities in the jet regions contained more high-frequency fluctuations and were more turbulent compared to those in the occupied regions. A higher diffuser air velocity resulted in more turbulent flow in the occupied regions. For the same diffuser air velocity, the thermal buoyancy effect due to the heat generated from the floor also contributed to the generation of turbulence in the occupied region.

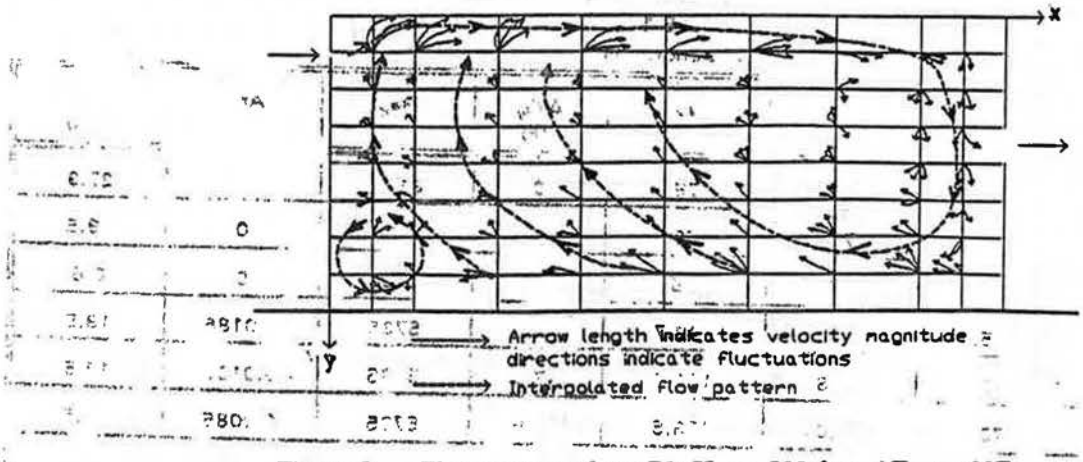

Figure 3 *Flow pattern of test P1:* U_d *= 500 fpm,* ΔT_{fd} *= 0°F.*

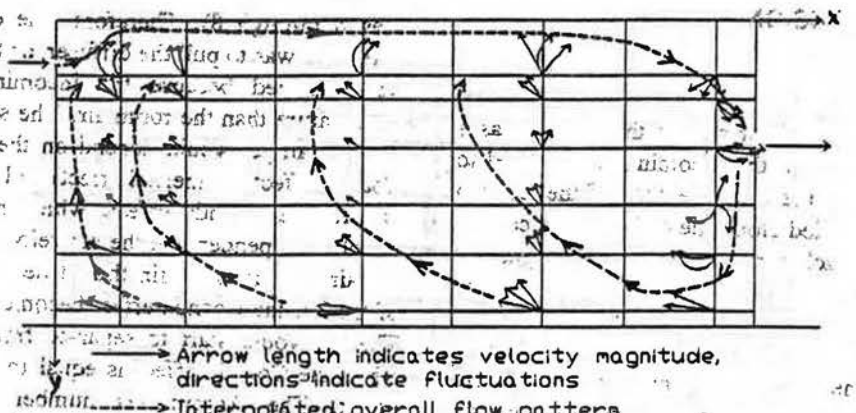

Figure 4 *Flow pattern of test P2:* U_d *= 350 fpm,* ΔT_{fd} *= 0°F.*

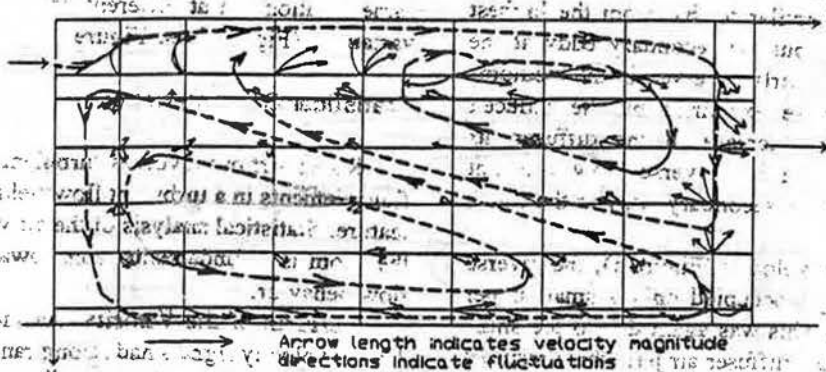

Figure 5 *Flow pattern of test P3:* U_d *= 150 fpm,* ΔT_{fd} *= 0°F.*

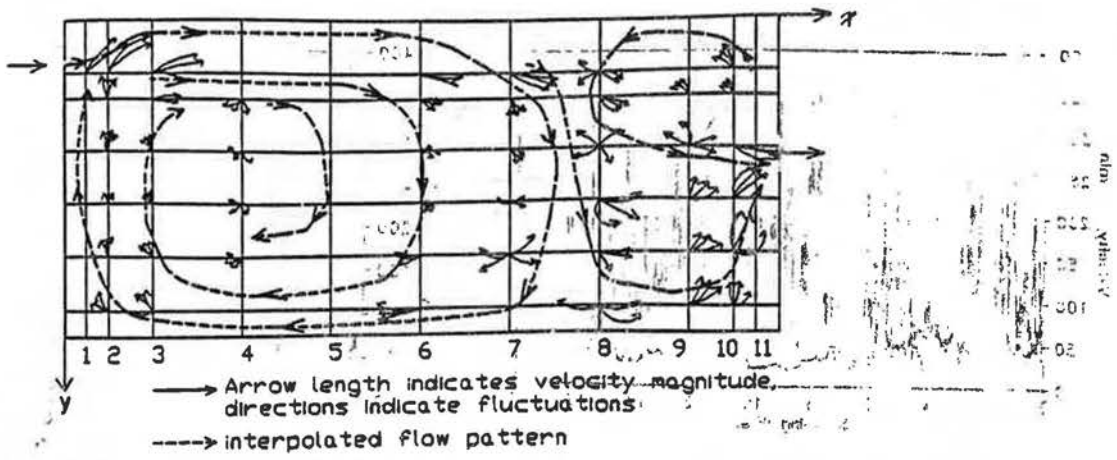

Figure 6 *Flow pattern of test P4:* $U_d = 350$ *fpm,* $\Delta T_{fd} = 67.3°F$.

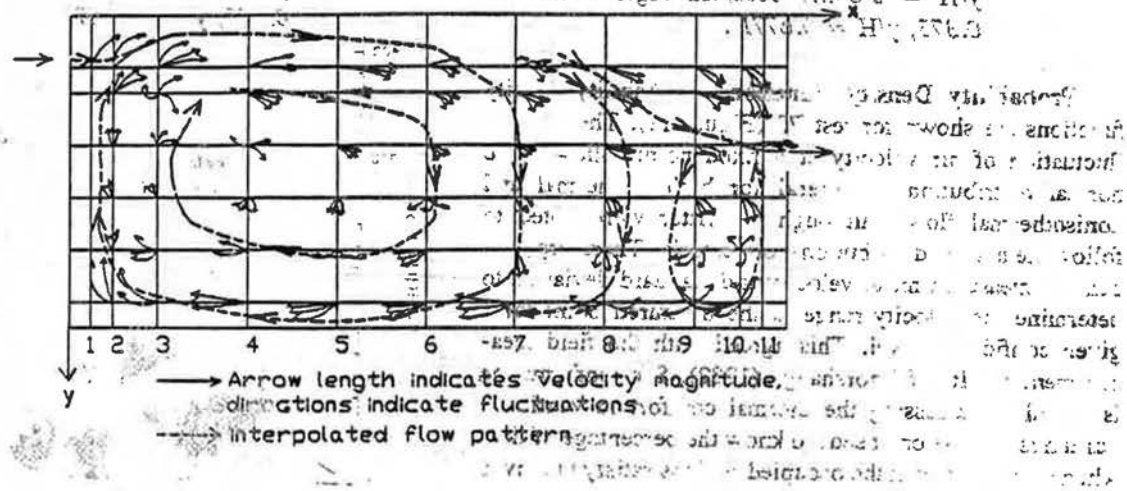

Figure 7 *Flow pattern of test P5:* $U_d = 350$ *fpm,* $\Delta T_{fd} = 47.9°F$.

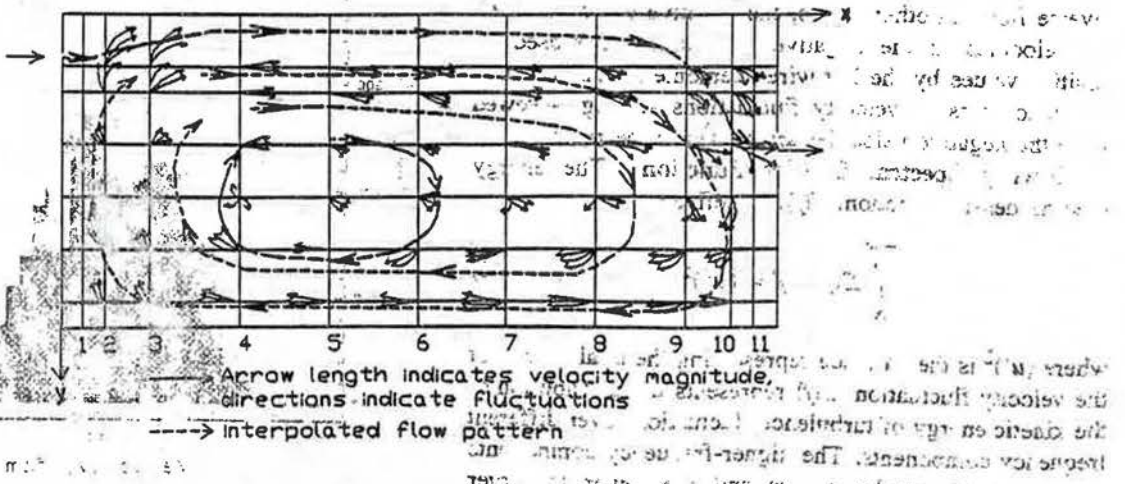

Figure 8 *Flow pattern of test P6:* $U_d = 350$ *fpm,* $\Delta T_{fd} = 29.6°F$.

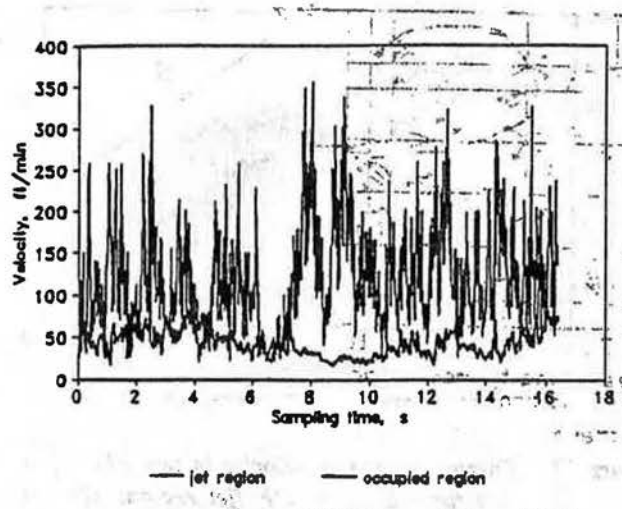

Figure 9 *Sample velocity signals in test P1: U_d = 500 fpm, ΔT_{fd} = 0°F (jet region: x/W = 0.125, y/H = 0.0521; occupied region: x/W = 0.375, y/H = 0.6771).*

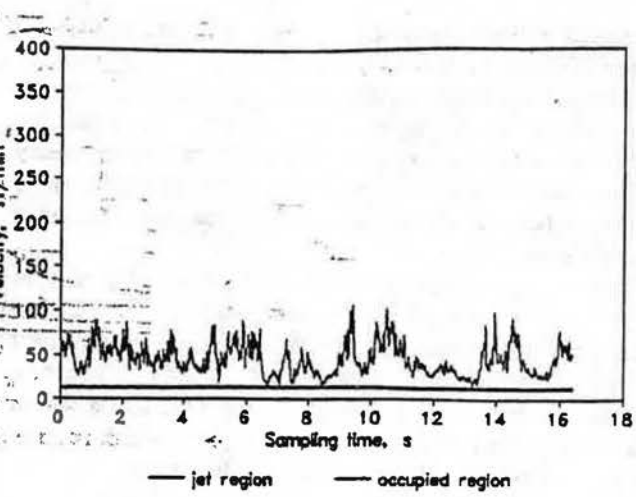

Figure 10 *Sample velocity signals in test P3: U_d = 150 fpm, ΔT_{fd} = 0°F (jet region: x/W = 0.125, y/H = 0.0521; occupied region: x/W = 0.375, y/H = 0.6771).*

Probability Density Function Probability density functions are shown for test P3 (Figure 11). The random fluctuation of air velocity at a fixed point followed the normal distribution in general for both isothermal and nonisothermal flows, although the latter were noted to follow the normal distribution more closely. Therefore, one can use measured mean velocity and standard deviation to determine the velocity range at the measured point for a given confidence level. This agreed with the field measurement results of Thorshauge (1982). Such information is useful for assessing the thermal comfort in ventilated buildings because one needs to know the percentage of time when air velocities in the occupied regions satisfy the given criterion.

The histograms of velocity fluctuations (Figure 11) are slightly right-skewed. This may be caused by the limitation of the hot-wire anemometer, which is unable to detect the reverse flow. In other words, the negative velocities (i.e., air velocities in the negative direction) are sensed as positive values by the hot-wire anemometer. As a result, the histograms of velocity fluctuations are right-skewed since the negative velocities are folded to the right.

Energy Spectral Density Function The energy spectral density function, $E(f)$, is defined as

$$\int_0^{+\infty} E(f)\,df = (u')^2 \qquad (1)$$

where $(u')^2$ is the variance representing the total energy of the velocity fluctuation. $E(f)$ represents the distribution of the kinetic energy of turbulence fluctuations over different frequency components. The higher-frequency components correspond to smaller eddies and the lower to larger eddies.

Velocities in the jet region contained higher levels of kinetic energy of turbulence compared to those in the

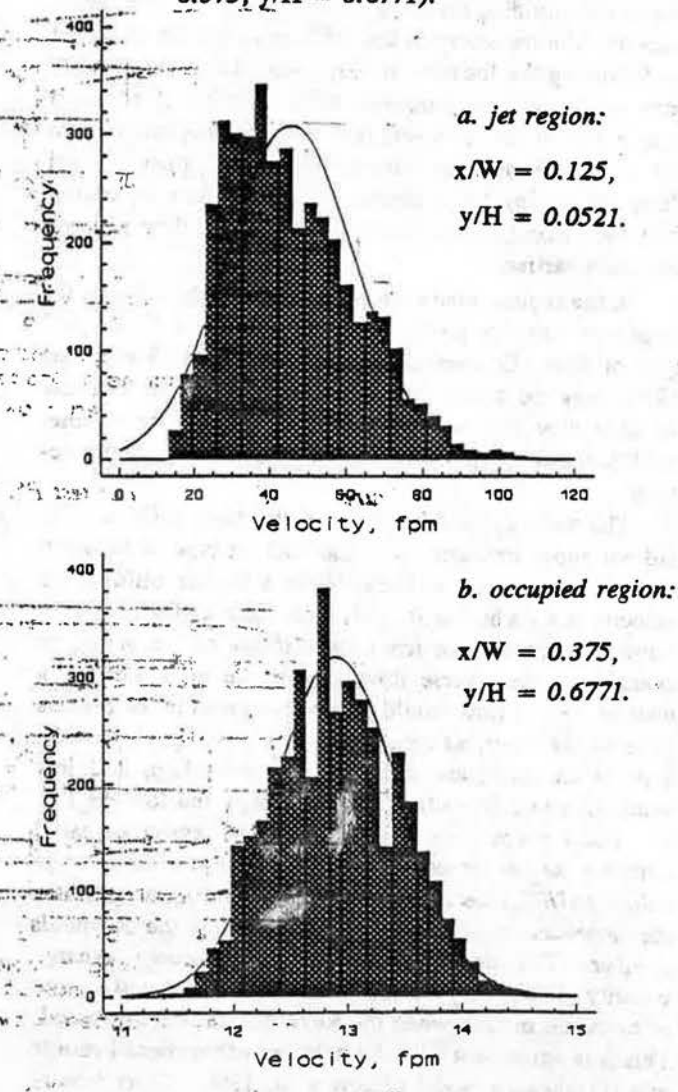

Figure 11 *Histograms of sample velocity signals in test P3: U_d = 150 fpm, ΔT_{fd} = 0°F.*

occupied regions, especially for the low-diffuser-velocity cases (Figures 12 and 13). The distribution also extended to higher frequencies for the jet regions. The large velocity gradients in the jet regions were mainly responsible for generation of turbulence according to the turbulence theory (Hinze 1975). High-velocity gradients also generated more small eddies, which corresponded to the high-frequency fluctuations.

It was also noted that thermal buoyancy due to heat production from the floor increased the turbulence energy in the occupied region, but had little effect on the turbulent kinetic energy in the jet region. Therefore, the contribution of thermal buoyancy to the turbulence production within the room is limited in the occupied region, which is close to the heat sources (floor surfaces in this case).

Mean Velocity

Spatial distributions of mean velocity are shown for test P6 (Figure 14), where all velocities are made dimensionless by dividing the local air velocity by the diffuser air velocity. The trajectory of the diffuser air jet can be traced by following the location at which the maximum velocity occurred in each measurement column (x/W). A common feature for all the tests was that the incoming air jet bent toward the ceiling after entering the room. It then traveled along the ceiling for a certain distance before separating from the ceiling again. This agrees with the flow patterns discussed earlier.

In the region where the jet attached to the ceiling, the measured velocity profiles were similar to a "wall jet" type of flow. Conventional wall jet theories (Schlichting 1979) may be tested with the present data to evaluate whether they adequately describe this region or whether modifications are necessary for acceptably accurate predictions.

The velocity profiles close to the floor ($y/H \geq .75$) did not show similarity with the wall jet type of flow but were more or less uniform. With a higher diffuser air velocity (i.e., a higher Re_d) than the case studied, a higher remaining momentum from the diffuser air jet would be available to the reverse flow. Due to the surface effect, a wall jet type of flow would also be produced in the regions close to the floor, as reported by Jin and Ogilvie (1990). This is an important difference between high and low ventilation rate flows (i.e., between high and low Re_d).

The average velocity in the occupied region increased with the Re_d as expected, but the dimensionless average velocity (U/U_d) decreased (Table 2). This again indicates the dependence of the air distribution on the Reynolds number. The decrease of the dimensionless average velocity (U/U_d) may be explained by the increased degree of turbulent mixing when the Reynolds number increased. This is in agreement with the previous experimental results in a 1/12th-scale model (Zhang et al. 1990). Other researchers (e.g., Timmons 1984) showed that when the Reynolds number was larger than a threshold, the distribution

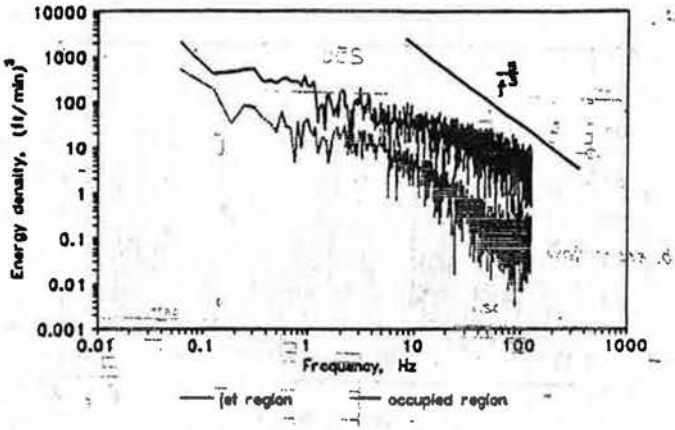

Figure 12 Energy spectra of velocity in test P1: U_d = 500 fpm, ΔT_{fd} = 0°F (jet region: x/W = 0.125, y/H = 0.0521; occupied region: x/W = 0.375, y/H = 0.6771).

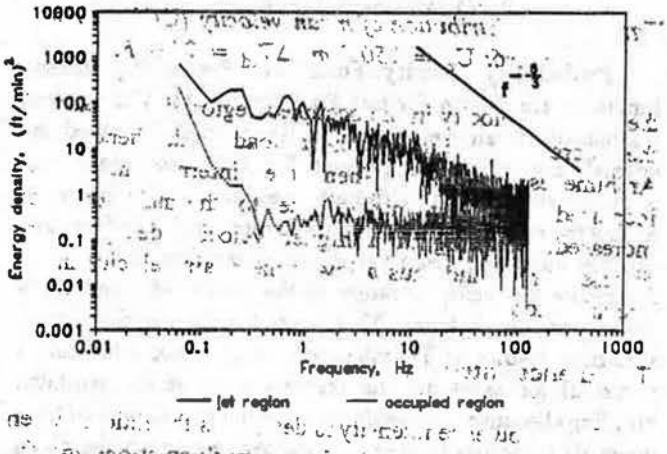

Figure 13 Energy spectra of velocity in test P3: U_d = 150 fpm, ΔT_{fd} = 0°F (jet region: x/W = 0.125, y/H = 0.0521; occupied region: x/W = 0.375, y/H = 0.6771).

of mean air velocity within a ventilated room became independent of the Reynolds number, and the threshold value increased with the room scale. However, most realistic room ventilation flows have Reynolds numbers well below the threshold, as in the present study. Therefore, the dependence of room airflows on the Reynolds number has to be considered in the study of realistic room ventilation flows.

Increasing the thermal buoyancy effect decreased the distance the air jet traveled along the ceiling and also made the jet expand faster. When the jet fell, it produced a region with relatively high air velocities in some part of the occupied region.

The average velocity in the occupied region was higher in the nonisothermal case than in the isothermal case since the diffuser air jet dropped directly to the occupied region (Table 3). However, for the three nonisothermal test cases,

a. jet region:

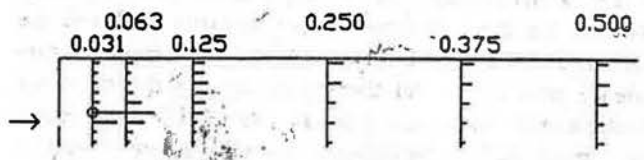

b. entire flow field:

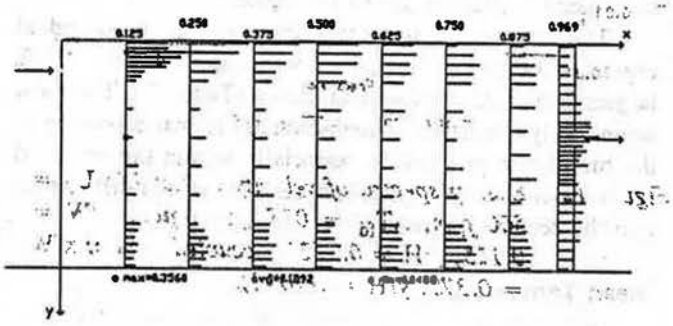

Figure 14 *Distribution of mean velocity (U/U_d) for test P6: U_d = 350 fpm, ΔT_{fd} = 29.6°F.*

the average velocity in the occupied region decreased with the increase of internal heat load and, hence, the Archimedes number. When the internal heat load increased, turbulent mixing due to thermal buoyancy increased, resulting in a higher velocity decay in the diffuser air jet and thus a lower mean air velocity in the occupied zone.

Turbulence Intensity

The turbulence intensity is defined as the ratio between the standard deviation (u') of velocity fluctuations and the mean velocity (U). It represents the degree of turbulence at a local point.

The distribution patterns of the turbulence intensity within the test room were not as apparent as in the mean velocity distribution (Figure 15). In general, relatively high values were distributed in the intermittent region at the edge of the diffuser air jet and at the central region of the recirculation eddy.

TABLE 2
Dependence of Average Velocity in the Occupied Region on the Reynolds Number

U_d, fpm	Re_d	U, fpm	U/U_d	Test
150	2458	16.2	0.108	P3
350	5489	27.0	0.077	P2
500	8192	35.7	0.070	P1

The occupied region is defined as the space from the floor to a 6-foot-high level and 1 foot from each side wall, which corresponds to $0.25 \leq y/H \leq 1.0$ and $0.5 \leq x/W \leq 0.94$, respectively.

a. jet region:

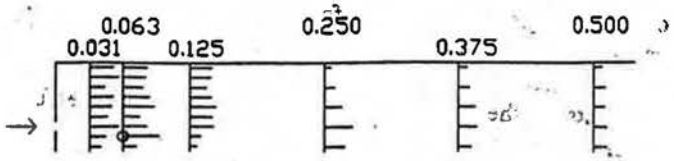

b. entire flow field:

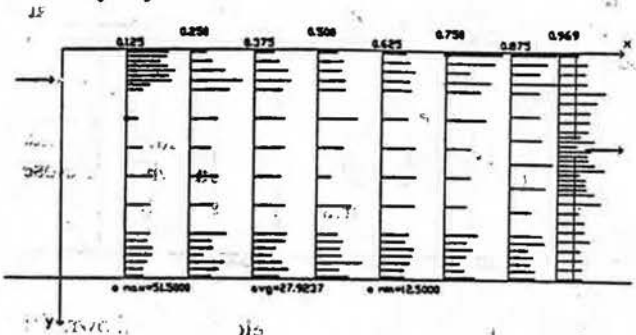

Figure 15 *Distribution of turbulence intensity (100 u'/U) for test P6: U_d = 350 fpm, ΔT_{fd} = 29.6°F.*

The average turbulence intensity in the occupied region increased with the increase of diffuser air velocity, as expected (Table 4). It also increased with the internal heat load because the thermal buoyancy caused the diffuser jet to drop into the occupied region and also contributed to the production of turbulence within the occupied region.

Turbulent Kinetic Energy

The kinetic energy of turbulence (k) is defined as 0.5 u'^2. It is a more appropriate term to represent the importance of the turbulence effect on the room air motion than turbulence intensity. The kinetic energy of turbulence in the diffuser jet region was substantially larger than in the occupied region (Figure 16), especially in the isothermal tests. Since the magnitude of turbulent kinetic energy in a local region depends on the turbulence generated within the region and that transported from upstream, one may infer

TABLE 3
Dependence of Average Velocity in the Occupied Region on the Archimedes Number

ΔT_{fd}, °F	Ar_{fd}	U, fpm	U/U_d	Test
0.0	0.0	27.0	0.077	P2
29.6	0.0085	35.4	0.101	P6
47.9	0.0135	33.5	0.098	P5
67.3	0.0196	29.0	0.084	P4

The occupied region is defined as the space from the floor to a 6-foot-high level and 1 foot from each side wall, which corresponds to $0.25 \leq y/H \leq 1.0$ and $0.5 \leq x/W \leq 0.94$, respectively.

a. jet region:

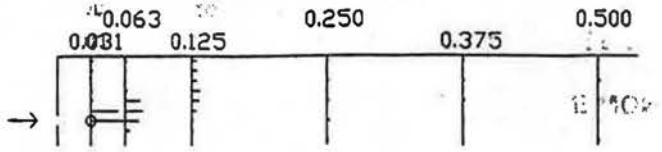

b. entire flow field:

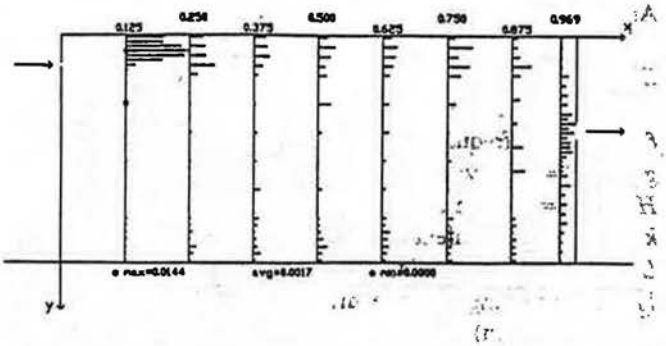

Figure 16 Distribution of turbulent kinetic energy ($k/0.5\ U_d^2$) for test P6: U_d = 350 fpm, ΔT_{fd} = 29.6°F.

that the turbulence within the room was mainly generated in the diffuser jet region due to the strong interaction between the incoming air and the room air and between the jet and the ceiling surface. The generated turbulence was then transported to the other parts of the room. In the transport process, the velocity fluctuations were also damped by viscous effects, resulting in lower turbulent kinetic energy in the occupied region. This phenomenon agrees with the turbulence theory (Hinze 1975), since large mean velocity gradients were present in the jet region but not in the occupied region.

The nondimensionalized turbulent kinetic energy of the occupied region was larger in the case of a higher diffuser velocity (Table 5). If the diffuser air velocity increases further, a sufficiently high-velocity gradient may be present between the solid surfaces of the opposite wall and the floor and the adjacent flow, resulting in significant turbulence production and thereby increasing the turbulent kinetic energy in the occupied region significantly. However, most realistic ventilation flows have low velocities (< 50 fpm) over the floor surface so that such additional turbulence production is negligible compared to the turbulence production in the jet region.

The average turbulent kinetic energy of the occupied region in nonisothermal flows was approximately 115% larger than in the isothermal flows (Table 5). This was again partly due to the contribution of thermal buoyancy to the turbulence production, especially within the occupied region itself, and partly due to the drop of the diffuser jet into the occupied region.

Mean Temperature

The distribution of mean temperature for the nonisothermal tests conducted was mainly determined by the mean velocity distribution (Figure 17). In other words, the temperature was lower upstream of the flow. As the air traveled, it was heated by the adjacent warmer air through turbulent mixing and molecular diffusion.

In the occupied region, the room air temperatures were much more uniform than the mean velocity distribution. This is mainly because the temperature field had different boundary conditions from the velocity field. Temperatures on the surfaces of the walls, ceiling, and floor were higher than (on the floor surface) or equal to (on other surfaces, assuming adiabatic conditions) the temperature of the air attached to the surfaces, while the air velocities on these surfaces were zero due to the air viscosity. Additionally, the molecular heat diffusion was faster than the molecular momentum diffusion since the Prandtl number of the air is

TABLE 4
Average Turbulence Intensity in the Occupied Region

U_d, fpm	Re_d	T_{fd}, °F	Ar_{fd}	u'/U_d, %	Test
150	2458	0	0	6.5	P3
350	5489	0	0	23.6	P2
500	8192	0	0	27.9	P1
350	5489	29.6	0.0085	26.1	P6
350	5489	47.9	0.0135	29.9	P5
350	5489	67.3	0.0186	33.9	P4

*The occupied region is defined as the space from the floor to a 6-foot-high level and 1 foot from each side wall, which corresponds to $0.25 < y/H < 1.0$ and $0.5 < x/W < 0.94$, respectively.

TABLE 5
Average Kinetic Energy of Turbulence in the Occupied Region*

U_d, fpm	Re_d	T_{fd}, °F	Ar_{fd}	$k/(0.5\ U_d^2)$,	Test
150	2458	0	0	0.00009	P3
350	5489	0	0	0.00042	P2
500	8192	0	0	0.00044	P1
350	5489	29.6	0.0085	0.00082	P6
350	5489	47.9	0.0135	0.00098	P5
350	5489	67.3	0.0186	0.00092	P4

*The occupied region is defined as the space from the floor to a 6-foot-high level and 1 foot from each side wall, which corresponds to $0.25 < y/H < 1.0$ and $0.56 < x/W < 0.94$, respectively.

a. jet region:

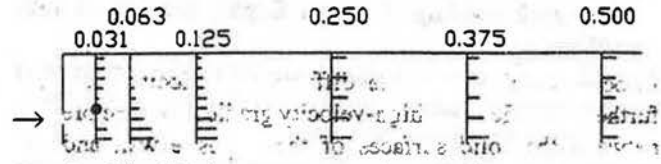

b. entire flow field:

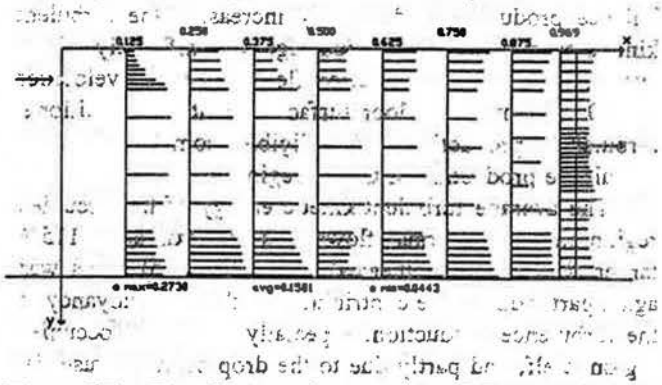

Figure 17 Distribution of temperature [(T − T_d)/ΔT_fd]h for test P6: U_d = 350 fpm, ΔT_fd = 29.6°F.

about 0.7. The Prandtl number represents the ratio between the momentum and thermal diffusion rates due to molecular motion (Kays and Crawford 1980).

SUMMARY AND CONCLUSIONS

1. Turbulence of room ventilation flows is mainly generated by the diffuser air jet. The turbulent kinetic energy in the occupied regions is significantly smaller and is distributed in a lower frequency range than in the diffuser jet region.
2. Normal distribution can be used to approximate the velocity fluctuations in the room ventilation flow.
3. Air distribution in realistic isothermal ventilation flows is dependent on the Reynolds number. Increasing the Reynolds number (Re_d) decreases the dimensionless average velocity ($\bar{U}/U_d$) and increases the turbulent kinetic energy and turbulence intensity in the occupied region.
4. The internal heat load may have significant effects on the room air distribution, causing the diffuser air jet to fall more quickly after entering the room. This causes a higher spatial average of mean velocity in the occupied region for the nonisothermal cases compared to the isothermal case under the same diffuser air velocity. The thermal buoyancy also contributes to the turbulence production within the room and thereby increases the turbulent kinetic energy and turbulence intensity in the occupied region.

The detailed measurements of distributions of air velocity, turbulent kinetic energy, and turbulence intensity are also useful for evaluating numerical simulation models.

ACKNOWLEDGMENT

This study was sponsored by the U.S. National Science Foundation and the University of Illinois Campus Research Board. Their financial support is highly appreciated. The authors are also grateful for the help of Jolien de Vos, Steve Ford, and Bo Zhang in conducting the experiments.

NOMENCLATURE

ach	=	air changes per hour
Ar_{fd}	=	Archimedes number, defined as $\beta g w_d (T_f - T_d)/U_d^2$
$E(f)$	=	spectral density function of velocity fluctuations, fpm^2 $(m/s)^2$
f	=	frequency, Hz
g	=	gravitational acceleration rate, fpm^2 $(m/s)^2$
H	=	room height, ft (m)
k	=	turbulent kinetic energy, fpm^2 $(m/s)^2$
L	=	length of the room (in Z direction), ft (m)
l_d	=	length of the diffuser slot (in Z direction), ft (m)
Q	=	ventilation rate, ft^3/min (m^3/s)
Re	=	Reynolds number, defined as $U_d w_d/\nu$
T_f	=	maximum temperature in room (e.g., on the heated surface), °F (°C)
T_d	=	diffuser air temperature, °F (°C)
T_e	=	air temperature at the exhaust, °F (°C)
ΔT_{ed}	=	$T_e - T_d$, °F (°C)
ΔT_{fd}	=	$T_f - T_d$, °F (°C)
u'	=	standard deviation of velocity, fpm (m/s)
U_d	=	reference velocity, diffuser velocity at the measurement plane ($z = 0$), fpm (m/s)
W	=	width of the test room (in X direction), ft (m)
w_d	=	width of the diffuser slot (in Y direction), ft (m)
w_e	=	slot width of the exhaust, ft (m)
x,y,z	=	Eulerian Cartesian coordinates, ft (m)
y_d	=	distance from the ceiling to the diffuser upper edge, ft (m)
y_e	=	distance from the ceiling to the upper edge of the exhaust, ft (m)
α	=	thermal diffusion coefficient, ft^2/min (m^2/s)
β	=	thermal expansion coefficient, 1/R (1/K)
ν	=	kinematic viscosity, ft^2/min (m^2/s)
ρ	=	density of diffuser air, lbm/ft^3 (kg/m^3)

REFERENCES

ASHRAE. 1989. *1989 ASHRAE handbook—Fundamentals.* Atlanta: American Society of Heating, Refrigerating, and Air-Conditioning Engineers, Inc.

Barber, E.M., S. Sokgansanj, W.P. Lampman, and J.R. Ogilvie. 1982. Stability of air flow patterns in ventilated spaces. ASAE Paper No. 82-4551.

Baturin, V.V. 1972. *Fundamentals of industrial ventilation*, 3d ed. Oxford: Pergamon Press.

Boon, C.R. 1978. Airflow patterns and temperature distribution in an experimental piggery. *J. Agric. Engng. Res.* 23(2): 129-139.

Carpenter, G.A., L.J. Moulsley, and J.M. Randall. 1972. Ventilation investigations using a section of a livestock building and airflow visualization by bubbles. *J. Agric. Engng. Res.* 17(4): 323-331.

Christianson, L.L. 1989. *Building systems: Room air and air contaminant distribution.* Atlanta: American Society of Heating, Refrigerating, and Air-Conditioning Engineers, Inc.

Fitzner, K.F. 1981. Airflow experiments in full-scale test rooms. *ASHRAE Transactions* 87(2): 1143-1153.

Hart, G.H., and D. Int-Hout. 1980. The performance of a continuous linear air diffuser in the perimeter zone of an office environment. *ASHRAE Transactions* 86(2): 107-124.

Hinze, J.O. 1975. *Turbulence.* New York: McGraw-Hill, Inc.

Jin, Y., and J.R. Ogilvie. 1990. Near floor air speeds from center slot air inlets in swine barns. ASAE Paper No. 904004. St. Joseph, MI: American Society of Agricultural Engineers.

Kays, W.M., and M.E. Crawford. 1980. *Convective heat and mass transfer.* New York: McGraw-Hill, Inc.

Melikov, A.K., H. Hanzawa, and P.O. Fanger. 1988. Airflow characteristics in the occupied zone of heated spaces without mechanical ventilation. *ASHRAE Transactions* 94(1): 52-70.

Miller, P.L., and R.G. Nevins. 1972. An analysis of performance of air distribution systems. *ASHRAE Transactions* 78(2): 191.

Murakami, S., and S. Kato. 1991. Numerical prediction of horizontal nonisothermal 3-D jet in room based on the k-ε model. *ASHRAE Transactions* 97(1).

Nevins, R.G., and P.L. Miller. 1972. Analysis, evaluation and comparison of room air distribution performance—A summary. *ASHRAE Transactions* 78(2): 235-242.

Ogilvie, J.R., and E.M. Barber. 1988. Jet momentum number: An index of air velocity at floor level. In *Building systems: Room air and air contaminant distribution*, ed. L.L. Christianson, pp. 211-214. Atlanta: American Society of Heating, Refrigerating, and Air-Conditioning Engineers, Inc.

Randall, J.M. 1975. The prediction of airflow patterns in livestock building. *J. Agric. Engng. Res.* 20(2): 199-215.

Randall, J.M., and V.A. Battams. 1979. Stability criteria for airflow patterns in livestock buildings. *J. Agric. Engng. Res.* 24(3): 361-374.

Sandberg, M. 1989. Velocity characteristics in mechanically ventilated office rooms. In *Room Vent '87, Proc. 1st International Conference of Air Distribution in Ventilated Spaces*, Session 2A, Stockholm, Sweden, 10-12 June.

Schlichting, H. 1979. *Boundary-layer theory.* New York: McGraw-Hill, Inc.

Straub, H.E., and M.M. Chen. 1957. Distribution of air within a room for year-round air-conditioning—Part II. University of Illinois Engineering Experiment Station Bulletin, No. 442. Urbana: University of Illinois.

Thorshauge, H. 1982. Air velocity fluctuations in the occupied zone of ventilated spaces. *ASHRAE Transactions* 88(2).

Timmons, M.B. 1984. Use of physical models to predict the fluid motion in slot-ventilated livestock structures. *ASAE Transactions* 27(2): 502-507.

Whittle, G.E., and E.M. Clancy. 1991. Evaluation of cases B,D,E—Presentation of results from measurements and simulations. IEA Annex 20 Research Report No. 1.22.

Wu, G.J., L.L. Christianson, J.S. Zhang, and G.L. Riskowski. 1990. Adjustable room ventilation simulator for room air and air contaminant distribution modeling. In *Indoor Air '90, Proc. 5th International Conference on Indoor Air Quality and Climate* 4: 237-242.

Zhang, J.S. 1991. A fundamental study of two dimensional room ventilation flows under isothermal and non-isothermal conditions. Ph.D. thesis, University of Illinois at Urbana-Champaign.

Zhang, J.S., L.L. Christianson, and G.L. Riskowski. 1990. Regional airflow characteristics in a mechanically ventilated room under nonisothermal conditions. *ASHRAE Transactions* 96(2).

Zhang, J.S., G.J. Wu, and L.L. Christianson. 1992. Detailed measurements of room air distribution for evaluating numerical simulation models. *ASHRAE Transactions* 98(1).